Study on Change Detection for Multi-temporal Polarimetric SAR Images

Zhang Juntuan[1,2,3]
[1] Texas Instruments-Jilin University DSPs Laboratory, Jilin University, 130026, Changchun, P. R. China
Zhang_juntuan@163.com

Huang shiqi[3]
[3] Xi'an Research Inst. of Hi-Tech, Hongqing Town, 710025, Xi'an, P. R. China
hshiqi@sina.com

LI Zhenfu[2]
[2] Xi'an Communication Institute, Xi'an, 710106, Xi'an, P. R. China
Lzf88ly@sohu.com

Lin Jun[1]
[1] Texas Instruments-Jilin University DSPs Laboratory, Jilin University, 130026, Changchun, P. R. China
lin_jun@jlu.edu.cn

***Abstract*—Multi-temporal single polarimetric synthetic aperture radar (SAR) images are performed change detection and it doesn't wholly reflect the change information of ground objects. Through analyzing the features of multi-polarimetric SAR images, the results show that the multi-polarimetric SAR image change detection ought to choose different polarimetric data, polarimetric total power data or echo polarimetric power ratio data in terms of different purpose and the effect of the former two states is better. Finally, the difference value two-threshold method is performed the change detection experiments with the multi-polarimetric data of Convair-580 C/X-SAR of Canada, and the experimental results obtain the expectant effect.**

***Keywords*—multi-temporal, polarimetric SAR images, change detection**

I. INTRODUCTION

Remote sensing image change detection is to understand and analyze the obtained different date images of the interested area and to provide a great deal of useful change information. It supplies reliable data source for area dynamic surveillance and topographic mapping database update, as reduces large numbers of manual operations. At present, change detection techniques have been successfully applied in many fields, such as environmental surveillance [1], forest change surveillance [2], disaster valuation [3], agricultural investigation[4][5], town extension surveillance[6][7], land utilization dynamic surveillance[8].

SAR image change detection techniques mainly focus on single polarimetric multi-temporal change detection. The traditional single channel and single polarimetric synthetic aperture radar can only obtain object scattering features of ground scene under a certain polarization sent-received combination, so that it obtains information is very limited. But multi-polarization SAR images can provide more abundant object scattering information. With the delivery of full polarization SAR satellite, for example, Japanese ALOS, Canadian Radarsat-2 and German Terra SAR-X, using polarimetric SAR image to perform quantitative remote sensing analyses and change detection for the complex earth surface is an important aspect for SAR application. Now polarimetric SAR data that is used in change detection is main pre-classification and post-detection [9][10][11], namely, using the physics scattering mechanism of objects to classify. This paper analyzes the scattering theory models of multi-polarization SAR data and the features of multi-polarization SAR images, and deep studies the change detection methods for multi-temporal polarimetric SAR images and finally performs test experiments with real measure data.

II. SAR DATA POLARIZATION THEORY

What single polarimetric SAR measures is the effective radar scattering section (RCS), but what full polarimetric SAR measures is the scattering matrix of the object. The polarimetric scattering matrix is usually called Sinclair scattering matrix. It unifies the energy feature, phase feature and polarimetric feature of object scattering and it perfectly describes the electromagnetic scattering characteristic of the radar targets.

According to the linear property of electromagnetic scattering, defining a complex polarization scattering matrix describes the change relation among each polarimetric component between incidence wave and far area scattering wave [12]. It is given by

$$E_{sc} = G(r)SE_{inc} \tag{1}$$

Where $G(r)$ is called spherical wave gene, S is a polarimetric scattering matrix of an object. E_{sc} and E_{inc} is expressed by vector form, then

$$E_{sc} = \begin{bmatrix} E_{sx'} \\ E_{sy'} \end{bmatrix}, \quad E_{inc} = \begin{bmatrix} E_{ix} \\ E_{iy} \end{bmatrix} \tag{2}$$

The polarimetric scattering matrix can be written by

$$S = \begin{bmatrix} S_{x'x} & S_{x'y} \\ S_{y'x} & S_{y'y} \end{bmatrix} \tag{3}$$

Where, S_{xy} is the target backscattering coefficient, which is sent by y polarization and is received by x polarization. Here, the relation between scattering matrix element and RCS is

$$\sigma_{ij} = 4\pi r^2 \left| s_{ij} \right|^2 \tag{4}$$

If the spherical wave gene $G(r)$ of the scattering matrix is defined by

$$G(r) = \frac{1}{\sqrt{4\pi}r} \tag{5}$$

Then the relation of scattering matrix element and RCS becomes

$$\sigma_{ij} = |s_{ij}|^2 \tag{6}$$

In BSA coordinate system, if choose (H,V) polarization base, the target complex scattering matrix that is measured by full polarization SAR can given by

$$S = \begin{bmatrix} s_{hh} & s_{hv} \\ s_{vh} & s_{vv} \end{bmatrix} \tag{7}$$

Under single station condition, the backscattering of a target has mutual exchange, namely, $s_{hv} = s_{vh}$. So the polarimetric matrix only have three independent elements, which can be written into a polarimetric scattering vector $X = [s_{hh} \quad s_{hv} \quad s_{vv}]^T$, and its covariance matrix is given by [13]

$$C = \left\langle XX^H \right\rangle = \begin{bmatrix} \left\langle s_{hh}s_{hh}^* \right\rangle & \left\langle s_{hh}s_{hv}^* \right\rangle & \left\langle s_{hh}s_{vv}^* \right\rangle \\ \left\langle s_{hv}s_{hh}^* \right\rangle & \left\langle s_{hv}s_{hv}^* \right\rangle & \left\langle s_{hv}s_{vv}^* \right\rangle \\ \left\langle s_{vv}s_{hh}^* \right\rangle & \left\langle s_{vv}s_{hv}^* \right\rangle & \left\langle s_{vv}s_{vv}^* \right\rangle \end{bmatrix} \tag{8}$$

Where, superscript H denotes conjugate transpose, $\langle\ \rangle$ denotes mean, * denotes complex conjugate.

At present, the applications of polarimetric SAR data are main to measure the covariance matrix and the scattering matrix of the target, and they are used to research the statistical characteristic, scattering mechanism and classification for the target [5][9][14][15].

III. EXPERIMENTAL DATA EXPLANATION

The polarization covariance matrix C can derive scattering matrix S , then the target polarization backscattering coefficients can be obtained by equation (6). The scattering coefficients turn into amplitude or intensity images. There are four different polarization combination forms for radar images, which are HH, HV, VH and VV. Fig.1 shows the polarimetric SAR images of Canadian Convair-580 C/X-SAR C-band. The imaging area is agricultural field, and the captured time is May 22 and 25, 1990. Where, Fig.1(a) is the single polarimetric SAR image of May 22 and Fig.1(b) is the single polarimetric SAR image of May 25.

(a) The single polarimetric SAR image of May 22

(b) The single polarimetric SAR image of May 25

Figure 1. The single polarimetric SAR images

IV. THE FEATURES AND CHANGE DETECTION OF POLARIMETRIC SAR IMAGES

A. *PolarizationTotal Power (Span) Map and Change Detection*

The polarization scattering total power stands for the measured total polarimetric scattering intensity, and the numerical value is the Span norm value of the target scattering matrix. Therefore, the polarization total power map is also called Span map, and it can be computed by

$$Span = |s_{hh}|^2 + 2\cdot|s_{hv}|^2 + |s_{vv}|^2 \tag{9}$$

Where, we assume that the target is mutual exchange, namely, $s_{hv} = s_{vh}$. The polarimetric scattering total power reflects the electromagnetic scattering characteristic of the target as a whole, and the numerical value is equal to the first element m_{00} of the Stokes matrix (or Mueller matrix) of the target. Fig.2(a) is the Span map of May 22 and Fig.2(b) is Span map of May 25. The polarization total power image fuses single polarimetric image, so full polarimetric power image can provide more details and the contrast of the image is stronger. The change detection results of the polarization total power image are shown in Fig.2. Where, Fig.2(c) is the change weakened area image and Fig.2(d) is the change enhanced area image.

Although the polarization total power image can detect the change information, it doesn't know which polarimetric form provides the change information. Single polarization change detection can reflect change types through the polarimetric scattering mechanism of ground objects. If the target area is known in advance, only detecting whether or not change, the polarization total power image can be used to perform change detection. Comparing with the change detection of the single polarimetric image, it reduces the calculated amount.

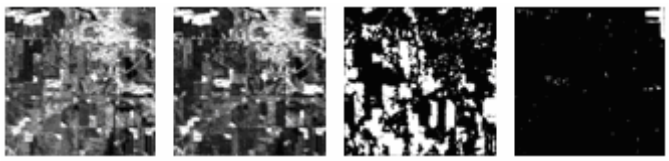

(a) (b) (c) (d)

Figure 2. The change detection results for the polarization total power image

B. *The Echo Power Ratio of Differ ent Polarization Image and Change Detection*

We can compute the polarimetric echo power ratio under the random polarimetric state, which is in favor of analyzing

the change instances of the relative echo power for different ground objects under different polarization combination. The definition of three different polarization echo power ratio is given by

$$\begin{cases} R_{hh/vv} = \dfrac{s_{hh}s_{hh}^*}{s_{vv}s_{vv}^*} = \dfrac{|s_{hh}|^2}{|s_{vv}|^2} = \dfrac{\sigma_{hh}}{\sigma_{vv}} \\ R_{hv/hh} = \dfrac{s_{hv}s_{hv}^*}{s_{hh}s_{hh}^*} = \dfrac{|s_{hv}|^2}{|s_{hh}|^2} = \dfrac{\sigma_{hv}}{\sigma_{hh}} \\ R_{hv/vv} = \dfrac{s_{hv}s_{hv}^*}{s_{vv}s_{vv}^*} = \dfrac{|s_{hv}|^2}{|s_{vv}|^2} = \dfrac{\sigma_{hv}}{\sigma_{vv}} \end{cases} \tag{10}$$

Fig.3 shows the power ratio of three polarimetric images which is shown in Fig.1(a). Where, Fig.3(a) is the same polarization power ratio, namely, it is the intensity ratio of HH and VV polarization. Fig.3(b) and Fig.3(c) are the echo intensity ratio of across polarization HV and same polarization HH or VV, respectively. The gray value of the pixel in Fig.3 is direct proportion with the echo power ratio under two polarizations in the area.

(a) $R_{hh/vv}$ (b) $R_{hv/hh}$ (c) $R_{hv/vv}$

Figure 3. The echo intensity ratio image of polarimetric images

It can see from Fig.3 that the echo power ratio is bigger of the same polarization HH and VV and that the echo power ratio is smaller of the across polarization HV and the same polarization HH or VV from Fig.3. Because VV polarization combines the crop structure, the vertical line is brighter in the HH/VV power ratio value image; on the contrary, the horizontal line is brighter in the HV/HH power ratio value image.

After the characteristic analysis for the polarimetric image echo power ratio, it is known that the power ratio image of the across polarization HV and the same polarization HH or VV can be performed change detection. The change detection results are shown in Fig.4. In experiment, because the same polarization power ratio image doesn't detect any change, Fig.4 only shows the change detection results of the power ratio image of the across polarization HV and the same polarization VV. Fig.4(a) is the power ratio image of HV/HH on May 22, Fig.4(b) is the power ratio image of HV/HH on May 25, Fig.4(c) is the change reduced area and Fig.4(d) is the change enhanced area.

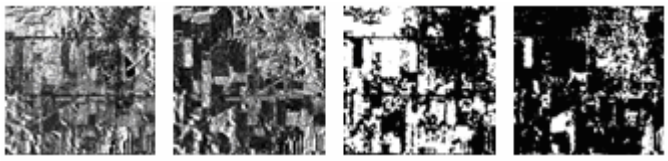

(a) (b) (c) (d)

Figure 4. The change detection results of the echo power ratio image

C. The Coherence of the Different Polarimetric Images

Multi-polarimetric SAR is a multi-channel system, and it can obtain the polarimetric scattering matrix and other correlative information for the ground objects. As provides vigorous instruments for us to analyze and understand the scattering characteristic of the ground objects. The polarimetric scattering matrix records the scattering characteristic of the ground objects: amplitude and phase. For mutual exchange medium, the polarimetric scattering matrix only has three independent parameters, which are HH, HV and VV. In order to better understand full polarization SAR images, we need know the relation between data that is measured by three independent channels. Therefore, we will study the relation between the three polarimetric image data.

The polarimetric SAR image relation can be expressed by the complex polarization covariance matrix C and the computed formula is given by

$$\begin{aligned} C_{kl} &= \left\langle s_k s_l^* \right\rangle \\ &= \begin{bmatrix} \sigma_1 & \rho_{12}\sqrt{\sigma_1\sigma_2} & \rho_{13}\sqrt{\sigma_1\sigma_3} \\ \rho_{12}^*\sqrt{\sigma_1\sigma_2} & \sigma_2 & \rho_{23}\sqrt{\sigma_2\sigma_3} \\ \rho_{13}^*\sqrt{\sigma_1\sigma_3} & \rho_{23}^*\sqrt{\sigma_2\sigma_3} & \sigma_3 \end{bmatrix} \end{aligned} \tag{11}$$

Where k and l denote the $k\ th$ and the $l\ th$ channel, respectively. $\sigma_k = \left\langle |s_k|^2 \right\rangle$ is the backscattering coefficient of the $k\ th$ independent channel. ρ_{kl} is the complex correlative coefficient between the $k\ th$ and the $l\ th$ channel, and it is computed by

$$\rho_{kl} = \frac{\left\langle s_k s_l^* \right\rangle}{\sqrt{\sigma_k \sigma_l}} \tag{12}$$

In practical application, because the scattering matrix date which we obtain has been transformed into the echo intensity image data and they are not the complex data, such as Fig.1 shows the original polarization SAR image, we can use equation (13) to compute the correlation of their polarization images.

$$\rho_{12} = \frac{\sum_{i=1}^{M}\sum_{j=1}^{N}\left[X_1(i,j)-\bar{X}_1\right]\left[X_2(i,j)-\bar{X}_2\right]}{\sqrt{\sum_{i=1}^{M}\sum_{j=1}^{N}\left[X_1(i,j)-\bar{X}_1\right]^2}\cdot\sqrt{\sum_{i=1}^{M}\sum_{j=1}^{N}\left[X_2(i,j)-\bar{X}_2\right]^2}} \tag{13}$$

Where, $X_1(i,j)$ and $X_2(i,j)$ are a certain pixel value in different polarization image, respectively. $\overline{X}_1$ and $\overline{X}_2$ are the mean of all pixels in the sliding window, , respectively. $M \times N$ is the size of the sliding window. The polarization correlation images are shown in Fig.5.

(a) ρ_{hh-vv} (b) ρ_{hv-hh} (c) ρ_{hv-vv}

Figure 5. The correlation of the polarimetric images

It can be seen from Fig.5 that the correlations are not good between each image. In theory, the three polarimetric images come from three independent channels, so their correlation is very bad. Especially, the correlation between the same polarization and the across polarization is zero. In fact, there includes a little information, which is brought by system noise and other reasons.

V. CONCLUSIONS

This paper analyzes the characteristic of the polarimetric SAR images and makes change detection for the multi-temporal polarization SAR images with difference value method in terms of their characteristic. The different polarization form reflects the different scattering information, so for the same area multi-temporal single polarimetric SAR images, the change detections are different. In practical application, choosing the corresponding polarimetric SAR images performs change detection according to the prior knowledge. This paper considers the change detection problems for the multi-polarization SAR images from image gray value, and makes test experiments with real measured SAR image data, and the good results are obtained. This is much significance for polarimetric SAR image change detection and application.

REFERENCES

[1] P. S. Chavez and D. J..Mackinnon, "Automatic detection of vegetation changes in the southwestern United States using remotely sensed images," Photogrammetric Engineering & Remote Sensing, Vol. 60, No.5, pp.1285-1294, 1994.

[2] S. Quegan, T. L. Toan, J. J. Yu, F. Ribbes and N. Floury, "Multitemporal ERS SAR analysis applied to forest mapping," IEEE Transactions on Geoscience and Remote Sensing , Vol..38, No.2, pp. 741-753, 2000.

[3] K. Grover, S. Quegan and C C Freitas, "Quantitative estimation of tropical forest cover by SAR," IEEE Transactions on Geoscience and Remote Sensing, Vol..37, No.1, pp.479-490, 1999.

[4] L. Bruzzone and S B Serpico, "An iterative technique for the detection of land-cover transitions in multispectral remote-sensing images," IEEE Transactions on Geoscience and Remote Sensing, Vol..35, No.4, pp. 858-867, 1997.

[5] S. Henning, T. S. Morten and G. T. Anton, "Multitemporal C- and L-band polarimetric signatures of crops," IEEE Transactions on Geoscience and Remote Sensing, Vol..37, No.5, pp. 2413-2429, 1999.

[6] K. R. Merril and L. Jiajun, "A comparison of four algorithms for change detection in an urban environment," Remote Sensing Environment, Vol. 63, No.2, pp. 95-100, 1998.

[7] T. T. Lee and R. Florrence, "Rice crop and monitoring using ERS-1 data based on experiment and modeling results," IEEE Transactions on Geoscience and Remote Sensing, Vol..35, No.1, pp.41-55, 1997.

[8] H. Zhang, N. Shu amd G. Liu, "Application of multitemporal composition and classification to land use change detection," Geomatics and Information Science of Wuhan University, Vol.30, No.2, pp. 131-134, 2005.

[9] M. Gabriele, S. Sebastiano and V. Gianni, "Unsupervised change detection from multichannel SAR images," IEEE Transactions on Geoscience and Remote Sensing Letters, Vol. 4, No.2, pp. 278-282, 2007.

[10] Q. Muhtar, "Polarization state conformation and its application to change detection in polarimetric SAR data," IEEE Transactions on Geoscience and Remote Sensing Letters, Vol.1, No.4, pp. 304-308, 2004.

[11] X. Kang, C. Z. Han, F. Xu and Y. H. Wang, "Unsupervised classification of polarimetric SAR image using deorientation theory and complex Wishart distribution," Journal of Electronics & Information Technology, Vol.29, No.4, pp.822-826, 2007. (in Chinese)

[12] J. W. Zhuang, S. P. Xiao and X. S. Wang, "Radar polarization information processing and application," Beijing: defence industry publishing house, 1999.

[13] F. T. Ulaby and C. Elachi, "Radar polarimetry for geoscience applications," Norwood, MA: Artech, 1990.

[14] C. Knut, A, N, Allan, S, Jesper and S, Henning, "A test statistic in the complex Wishart distribution and its application to change detection in polarimetric SAR data," IEEE Transactions on Geoscience and Remote Sensing, Vol.41, No.1, pp. 4-19, 2003.

[15] B. W. Dai, "Study on polarimetric synthetic aperture radar system and polarimetric information processing," Beijing: Chinese Academy of Sciences doctor's degree theses, 2000.